LA-5711-PR
Progress Report

Special Distribution
Issued: August 1974

Quarterly Report

Joint Services Explosives Program

March 16 through June 30, 1974

Compiled by

A. Popolato

los alamos
scientific laboratory
of the University of California
LOS ALAMOS, NEW MEXICO 87544

UNITED STATES
ATOMIC ENERGY COMMISSION
CONTRACT W-7405-ENG. 36

This series of reports presents the status of the LASL Joint Services Explosives Program. Other reports in the series, all unclassified are:

LA-5402-PR
LA-5521-PR
LA-5616-PR

In the interest of prompt distribution, this progress report was not edited by the Technical Information staff.

This work was performed with funds provided by the Defense Advanced Research Projects Agency under DARPA Order No. 2502.

CONTENTS

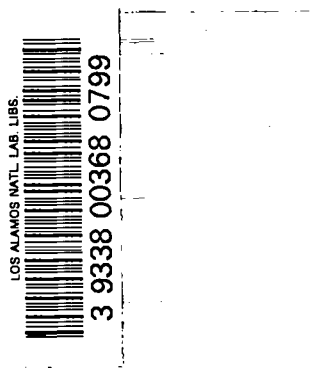

JOINT SERVICES EXPLOSIVE PROGRAM

QUARTERLY PROGRESS REPORT

FOR THE PERIOD MARCH 16 THROUGH JUNE 30, 1974

compiled by

A. Popolato

PREFACE

This is the fourth of a series of progress reports describing the status of four tasks undertaken by the Los Alamos Scientific Laboratory (LASL) for the Defense Advanced Research Projects Agency. The intent of LASL is to issue these reports on a quarterly basis. Since the tasks undertaken by LASL form an integral part of the Joint Services Explosive Program, copies of this report are being distributed to the agencies of the services participating in the program. Separate final reports will be issued for each of the tasks at the termination of each task.

ABSTRACT

The results obtained, for the period from March 16 through June 30, 1974, on the Joint Services Explosive Program are presented. The tasks undertaken by the Los Alamos Scientific Laboratory include: (1) Physical and Processing Characteristics of Nonideal Explosives - Special Emphasis on Amatex, (2) Analysis of Prematures, (3) Synthesis of HMX, and (4) Initiation and Sensitivity.

I. SUMMARY REPORT

A. PHYSICAL AND PROCESSING CHARACTERISTICS OF NONIDEAL EXPLOSIVES - SPECIAL EMPHASIS ON AMATEX (TASK A)

1. Introduction

The processing characteristics of Amatex [mixtures of RDX, TNT, and ammonium nitrate (AN)] have been determined as a function of composition and AN granulation. Preliminary data have been obtained on the shock initiation properties of Amatex/20. The experimental determination of relative energy of Amatex as a function of composition and AN granulation has been started.

Results of this work should provide a base line of engineering information that can be used by the munition designer and the process engineer to optimize the utilization of Amatex.

2. Progress This Report Period

a. Amatex Processing Study

The flow properties of Amatex melts have been determined as a function of composition and AN particle size distribution. For a constant

composition, the apparent viscosity increased exponentially as the median particle diameter of the AN was decreased. As the AN content was increased at the expense of RDX, with the TNT content maintained constant, the flow changed from Newtonian to plastic. The change from Newtonian to non-Newtonian flow depends upon the particle size distribution of the AN (or total AN surface area). The addition of nitrocellulose (NC) as a surface active agent significantly improves the flow properties. A minimum in the apparent viscosity of an Amatex melt prepared with NC occurred with the addition of 0.15 wt% NC. This quantity of NC added to Amatex does not have any significant effect on the thermal stability.

The significance of this finding is that, if granular AN is used in the preparation of Amatex, the AN particle size requirements can be significantly relaxed.

Amatex/20 or Amatex/40, prepared with prills in either a vacuum or open melt and cast at 83-88°C (normal casting temperatures), gives cast charges with large composition and density gradients. Uniform compositions and densities can be obtained if the temperature of the melt is reduced to the melting point of TNT, and TNT crystallization (nucleation or creaming) is induced before casting. This technique requires precision control of the melt temperature and viscosity. The density of Amatex/20 casting averages 1.57 g/cm^3 for "creamed" cast open melts and > 1.61 g/cm^3 for creamed cast vacuum melts.

Amatex/20 or Amatex/40, prepared with granular AN in either an open or a vacuum melt, can be cast with the procedures normally used for Composition B. The requirement for precision control of melt temperature and viscosity is eliminated.

The addition of 0.25 wt% anthracene to the Amatex melt was found to reduce the cracking tendencies of the cast pieces.

b. Amatex Properties

The failure diameter of Amatex/20 at room temperature in an unconfined geometry is 17 mm; Comp. B in a similar geometry fails at 2.1 mm.

Preliminary data on the shock sensitivity of Amatex/20 prepared with AN having a median particle diameter of 500 μm indicate that Amatex/20 is significantly less shock sensitive (more difficult to initiate) than Comp. B. These data indicate that the size of the booster required to initiate prompt detonation in the Amatex/20 charge must be larger than the booster used for Comp. B.

The energy of Amatex relative to Comp. B has been determined as a function of composition and AN particle size in terms of its ability to accelerate metal (copper cylinder test). In a 102-mm copper cylinder test, at a scaled expansion of 19 mm, Amatex/20 imparts 82% as much energy as Comp. B, and Amatex/40, 93%. These data are in agreement with data obtained by J. Hershkowitz, Picatinny Arsenal (PA). Preliminary results obtained with Amatex/20 prepared with prilled AN indicate that the relative energy is not significantly reduced.

3. Future Work

Work on the initiation characteristics and performance as a function of composition and granulation is in progress. The processing characteristics and properties of Amatex may be affected if mixtures of AN and potassium nitrate (KN) are used to replace AN. These changes should be small. We feel that some work should be done to determine the magnitude of the change. Work should be started to determine the optimum composition of KN in AN to minimize the growth of cast charges subjected to thermal cycles over the temperature range of military interest.

B. ANALYSIS OF PREMATURES (TASK B)

1. Introduction

Work on the thermal ignition model of initiation and attempts to calibrate the model with results of "aquarium" experiments is continuing.

2. Progress This Report Period

The results reported last quarter[1] of a one-dimensional analytical study designed to simulate the base gap closure initiation experiments conducted with the aquarium technique indicated that the generation of thermal energy, due to gas compression and its subsequent transfer to the HE and base plate, was not sufficient to initiate a thermal event. A new one-dimensional thermal transport program, developed by the University of Arizona with Air Force Office of Scientific Research (AFOSR) funds, was used to simulate the aquarium experiments. This program, NEWGAP, differs from the previous thermal transport program in one major respect. The mesh size is automatically adjusted to accommodate large thermal gradients. The results obtained with this calculation indicate that ignition is possible with base gaps of 1 mm filled with air or krypton. This is in agreement with experimental results.

3. Future Work

Additional aquarium tests will be performed with explosives having "defect free" surfaces. Polishing techniques are being developed in an effort to prepare these surfaces. Other initiation models, utilizing internal surface defects, and methods of concentrating energy in the defects will be tried to determine if sufficient thermal energy is generated to initiate ignition.

C. SYNTHESIS OF HMX (TASK C)

Funds allocated to this task were expended during the first two quarters, and results were reported in the first and second quarterly reports.

Additional work is being conducted with funds provided by PA.

D. INITIATION AND SENSITIVITY (TASK D)

1. Introduction

The ultimate objective of this investigation is to obtain a quantitative understanding of the mechanisms leading to the initiation of a violent reaction in the high explosive. One approach to developing a quantitative model of the initiation is to study the response of an explosive subjected to a single shock of known amplitude and duration in a one-dimensional system. This requires the development of a plane wave shock generator and supporting instrumentation for experiments that will generate data that can be used to determine the state of the shocked explosive as a function of time and initial conditions.

2. Progress This Report Period

Our problem to date has been the design of a satisfactory flyer plate plane wave generator. We have traced part of the problem related to the design of the flyer plate plane wave shock generator to the method used to bond the sheet explosive to the aluminum flyer. Small air gaps between the explosive and aluminum caused large timing errors. Techniques are being developed to improve the bonding procedure.

3. Future Work

Work will continue on the design of plane wave generators and the instrumentation required to measure the amplitude and duration of the shock pulse.

II. PROGRESS REPORT

A. PHYSICAL AND PROCESSING CHARACTERISTICS OF NONIDEAL EXPLOSIVES - SPECIAL EMPHASIS ON AMATEX (TASK A), A. W. Campbell, R. P. Engelke, A. Popolato, T. Rivera

1. Introduction

During the past quarter, we have continued to place our emphasis on the processing characteristics of Amatex. The melt flow properties have been determined as a function of composition, and AN particle size distribution, with and without a surface active agent (NC). Some data have been obtained on the casting properties and the shock initiation characteristics. The ability of Amatex to accelerate metal has been determined as a function of composition and AN granulation.

These data should provide part of the base line of information required by the munition designer

and process engineer to optimize the utilization of Amatex in munitions.

2. Progress This Report Period

a. Amatex Processing Study

(1) Flow Properties of Amatex Melts. The flow properties of Amatex melts have been determined as a function of AN particle size distribution and NC concentration. The purpose of this study was to determine the degree of process control required on the AN grinding operation.

All the melts were prepared as open melts with Comp. B Grade A meeting the requirements specified in MIL-C-401C, TNT meeting the requirements in JAN-T-248, and prilled AN meeting the requirements specified in MIL-A-50460. The apparent viscosities were determined with a modified Stormer rotational viscometer at a constant shear rate of 2 rps and at a constant shear stress equivalent to a driving weight of 200 g. The efflux viscosities were determined in accordance with the procedures specified in MIL-Std-650, Explosives Sampling, Inspection and Testing. The AN granulation was varied by adjusting the grinding conditions on a Model 5H Mikro Pulverizer hammer mill. A tabulation of the grinding conditions and the resulting AN particle size distribution is given in Table I.

The apparent viscosity of Amatex/20 and Amatex/40 as a function of AN particle size is shown in Fig. 1. Castable mixtures of Amatex/20 or Amatex/40 can be made without surface active agents with ground AN having a median particle diameter of ≥500 μm. As the median diameter is reduced, apparent viscosity increases exponentially. Neither Amatex/20 nor Amatex/40 can be prepared with AN ground to a median diameter of 50 μm without a surface active agent (NC). Amatex/20 or Amatex/40 prepared with AN having a median particle diameter of 200 μm and without a surface active agent (NC) can be cast at 85 to 90°C with difficulty.

The change in apparent viscosity of Amatex as a function of composition (by weight) and in which

TABLE I

AN PARTICLE SIZE DISTRIBUTION

Feed - AN prills per MIL-A-50460
Source - Terra Chemical International, Inc.
Feed rate - 9 kg/h
Hammer speed - 2960 rpm
No. of hammers - 3

Standard U.S. Sieve	Sieve Opening (μm)	Wt% AN Retained on Indicated Sieve Exit Screen Opening (mm) 1.19	3.75
16	1190	0	2.1
20	840	0.2	15.3
35	500	11.8	33.1
60	250	33.2	24.5
80	177	8.3	4.5
100	149	6.8	4.3
<100	<149	39.7	16.2
Median diameter (μm)		200	500

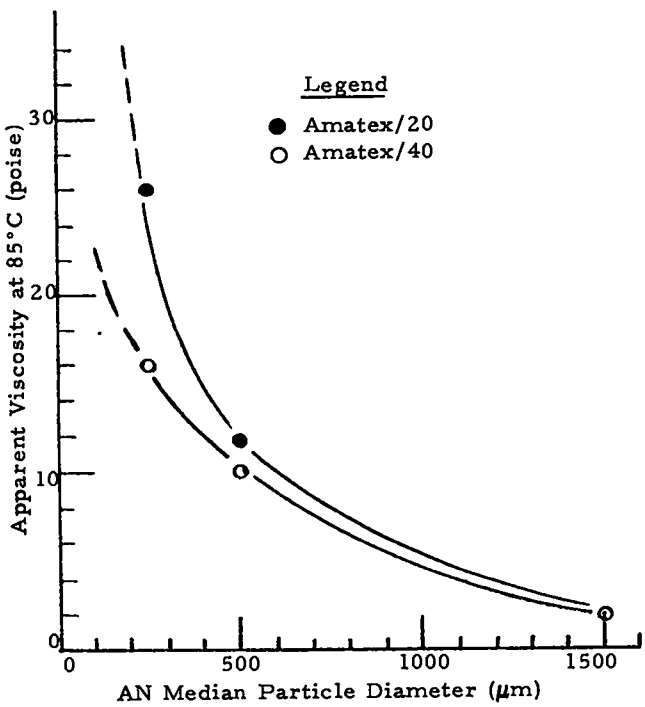

Fig. 1. Amatex viscosity as a function of AN median particle size.

AN replaces RDX and the TNT is maintained constant, is shown in Fig. 2. As AN replaces RDX, the apparent viscosity increases and in the limit, as all the RDX is replaced by AN (Amatol), non-castable mixtures are obtained with ground AN. This indicates that the TNT wets RDX much better than it wets AN. Another indication of this is shown in Fig. 3 in which the apparent viscosity of Amatex is displayed in the shear rate-shear stress plane. As the AN content is increased at the expense of RDX, the flow changes from Newtonian to non-Newtonian with a yield stress that continues to increase exponentially as the AN concentration increases. With granular AN having a median particle diameter of 200 μm, a yield stress appears at a composition equivalent to Amatex/40.

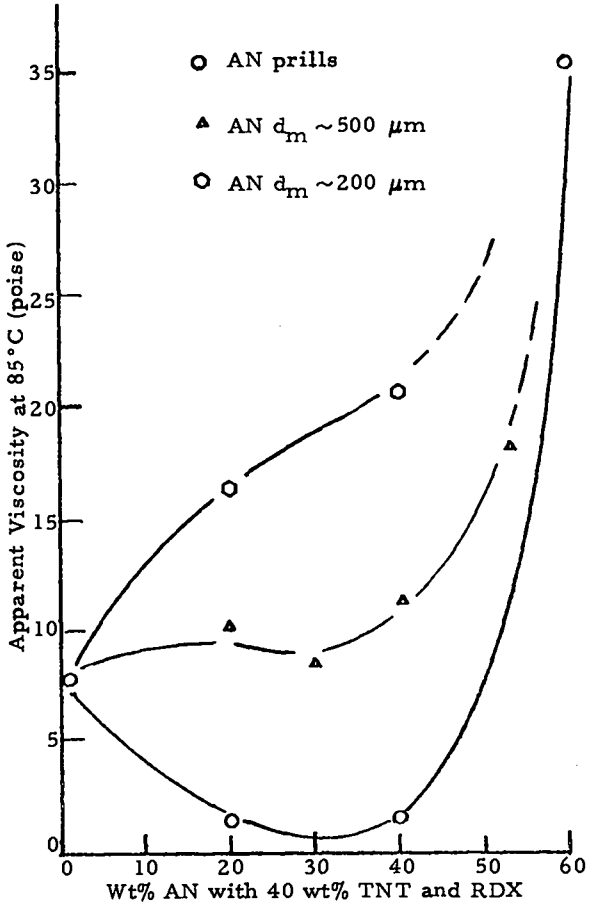

Fig. 2. Amatex viscosity as a function of composition and AN particle size distribution.

The appearance of a yield stress or the departure from Newtonian flow to plastic flow generally introduces casting problems. The effect of the addition of 0.15 wt% NC to Amatex melts is also shown in Fig. 3. In all cases, the yield stress (driving weight) is reduced significantly.

The effect of NC as a surface active agent is shown in Fig. 4, a plot of yield value as a function of composition and AN granulation. An important aspect of the family of curves shown in Fig. 4 from the standpoint of processing is to compare the yield value of Amatex/20 prepared with 500- and 200-μm AN and with and without 0.15 wt% NC. The yield value of Amatex/20 prepared with 200-μm AN was reduced from 110 to 10 g by the addition of 0.15 wt% NC. This is a significant reduction in yield that reflects itself in improved pour properties. Although castable mixtures of Amatex/20 can be prepared with either 500- or 200-μm AN, the addition of NC reduces the differences between the two melts, and improves the flow properties of Amatex/20 prepared with 200μm AN to the point where it can be poured without serious problems. With the addition of NC, large variations in AN granulation can be tolerated without introducing large variations in the casting properties of the melt.

The optimum amount of NC was determined with AN having a median particle diameter of 50 μm. Results of this study are shown in Fig. 5. A minimum was found at 0.15 wt% NC. The shape of the curve is characteristic of surface activity. The sharp reduction in viscosity is an indication of better interfacial wetting. The increasing viscosity, as the NC concentration is increased, is most likely due to the increased viscosity of the liquid TNT-NC solution.

(2) Casting Properties. A summary of the casting characteristics of Amatex is given in Table II.

The casting properties of Amatex/20 and Amatex/40 were determined as a function of AN granulation. Amatex charges 102 mm in diameter were

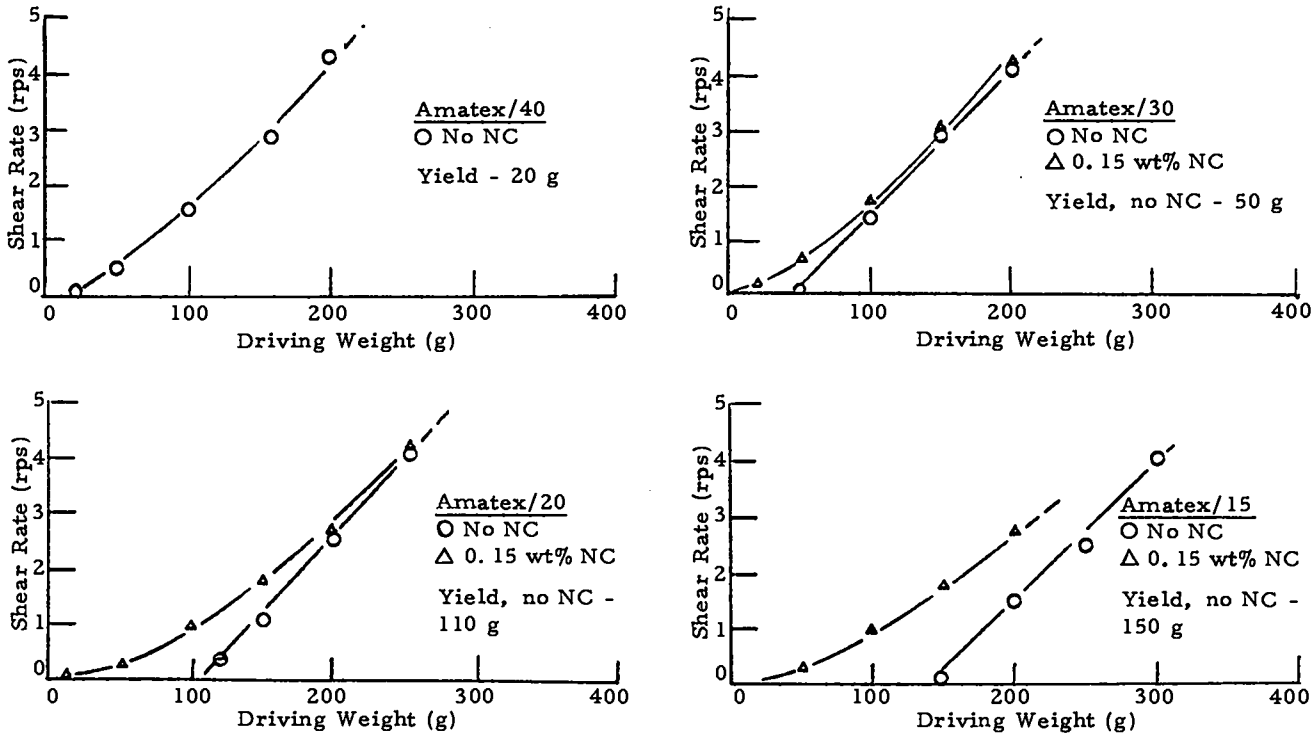

Fig. 3. Flow properties of Amatex at 85°C as a function of composition. AN median particle diameter: 200 μm.

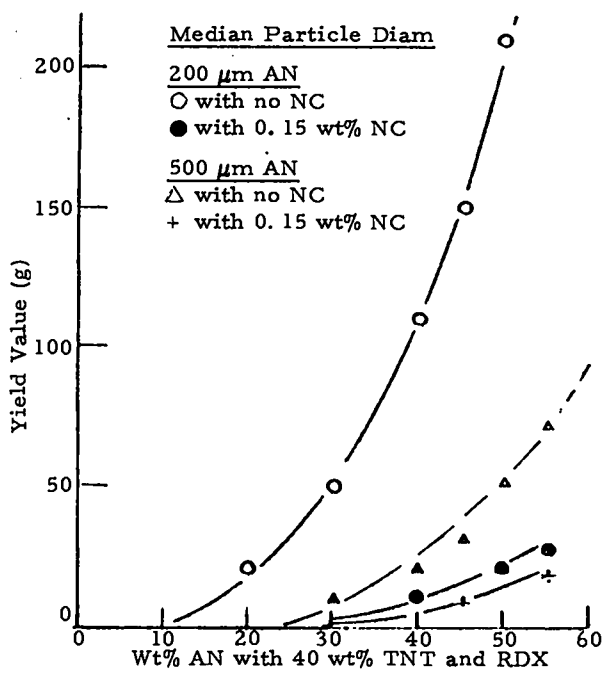

Fig. 4. Yield value of Amatex as a function of composition, AN particle size distribution, and NC surface active agent.

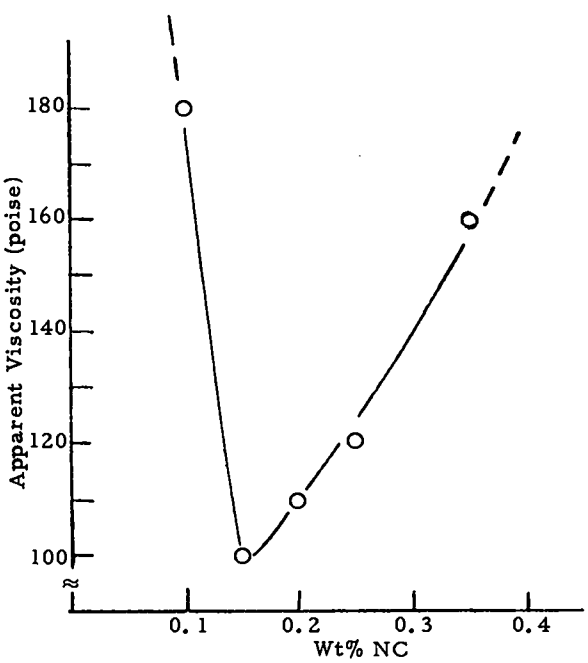

Fig. 5. Amatex/20: Effect of NC on apparent viscosity, AN $d_m \sim 50$ μm.

TABLE II

AMATEX CASTING SUMMARY[a]

Material	Type Melt	Casting Temperature (°C)	Efflux Viscosity (s)	Type AN	Charge Density (g/cm³)	Average Charge Composition (wt%) RDX	TNT	AN	Wax
Amatex/40	Open	84	6.2	Granular[b]	1.652	41.9	36.2	21.4	0.5
Amatex/40	Vacuum	84	3.0	Prilled	1.683	46.3	32.8	21.6	0.4
Amatex/20	Open	84	11.5	Granular	1.613	20.2	39.0	40.6	0.3
Amatex/20	Vacuum	84	3.0	Prilled	1.642	20.0	35.7	46.0	0.3
Amatex/20[c]	Open	84	3.0	Prilled	-	-	-	-	-
Amatex/20[c]	Open	79-80	6.0-14.0	Prilled	1.570	20.0	39.0	41.0	-

[a]Pieces cast were 101 mm diam by 150 mm high, mold preheat 90°C reduced to 84°C at pour and then reduced to 30°C after 30 min, riser 90°C at pour time reduced to RT after 2 h.

[b]Granular AN median particle diameter 500 μm.

[c]0.15 wt% NC added to melt.

cast to a height of 150 mm in aluminum molds. The lower 100 mm of the casting was sectioned and analyzed for density and composition. Results of this study are presented in Table II.

Amatex/20 or Amatex/40 prepared with prills in an open melt cannot be cast satisfactorily at a pour temperature of 84°C because the prills tend to segregate toward the upper portion of the casting. The addition of 0.15 wt% NC to Amatex prepared with prills in an open melt or the preparation of Amatex with prills in a vacuum melt prevents the segregation of prills to the riser. If these melts are cast at 84°C, the AN tends to segregate toward the base of the casting. Segregation can be prevented if the casting temperature is reduced to 79-80°C. At this temperature, TNT crystallization starts and the melt viscosity increases. Casting at the lower temperature requires precision control of the melt temperature and the degree of TNT creaming or crystallization. Another technique that has been used in loading plants to achieve the equivalent of creaming is to add TNT to the melt before pouring. We have not tried this. The maximum density that we were able to obtain in Amatex/20, prepared with prills and cast at 79 to 80°C, was 1.57 g/cm³. Amatex/20 or Amatex/40 prepared with granular AN (ground prills) in an open melt can be cast at 84°C. For Amatex/20, the average charge density is ≥1.61 g/cm³ and the charges are homogeneous.

From the standpoint of casting, our results indicate that the use of granular AN requires less process control. The melt temperature at casting can be varied from about 83 to 88°C without any significant changes in casting procedures or in the quality of the cast charge.

(3) Charge Cracking. With Amatex/40, we have observed cracking in the 102-mm-diam cast charges. The addition of 0.25 wt% anthracene to the melt eliminated the cracks. Anthracene was used by the Atomic Energy Commission to reduce the cracking tendency of TNT-based cast explosives without increasing the exudation problem.

The addition of anthracene did not change the flow properties of Amatex melts.

b. Shock Initiation of Amatex

The shock initiation of Amatex is a subject that has not received much systematic study. Necessary preliminaries are the establishment of the dependence of detonation velocity on charge diameter (the diameter-effect curve) and the determination of the failure diameter. With this information, one can more efficiently select boosters for initiation experiments and can better evaluate the observed initiation behavior of Amatex.

(1) Diameter Effect and Failure Diameter of Amatex/20. The diameter-effect curve for Amatex/20 prepared with AN having a median particle diameter of 500 μm was established by measuring the detonation velocity at each of four rate stick diameters using the technique described in Ref. 2. Detonation velocity data for the three larger diameters were obtained in previous work[a] as was an estimate of the failure diameter. During the past report period, the curve was completed with the firing of a rate stick with a diameter very close to failure diameter (17 mm).

All the rate sticks were initiated with plane wave lenses of appropriate diameter and with at least six diameters of self-booster, except for the 17-mm stick. In the case of the latter, the plane wave lens was followed by a 25-mm-diam section of Amatex/20 so as to slightly overboost the rate stick, which consisted of four sections each three diameters long.

The x-t data for the larger sticks were first fitted with the form

$$x = a_1 + b_1 t + c_1 t^2$$

using a least-squares program on a CDC 6600 computer. The result of this treatment was to show that the values of c, the acceleration, were either not statistically or physically significant. Since the acceleration term was not significant, the data were then fitted with a straight line,

$$x = a + bt \ .$$

Results of this fitting are listed in Table III.

TABLE III

DETONATION VELOCITY OF AMATEX/20[a]

Charge Diameter (mm)	No. of Segments	Booster Effect (mm) a	Booster Effect (mm) σ	Detonation Velocity (mm/μs) b	Detonation Velocity (mm/μs) σ	Charge Density (g/cm³)
101.6	13[b]	-0.733	0.147	6.937	0.0011	1.613
50.8	14[c]	0.130	0.039	6.833 6.840[d]	0.0006	1.611
25.4	10[e]	0.239	0.0445	6.542 6.532[d]	0.0013	1.616
17.0	2[f]	-	-	6.029	-	1.613

[a] Distance-time data were fitted with the form $x = a + bt$.

[b] Length of segment: 69.8 mm.

[c] Length of each segment: 50.8 mm.

[d] Detonation velocity corrected for density to $\rho = 1.613$ g/cm³ by use of $\Delta D/\Delta\rho = 3.5 \times 10^3$ (m/s)/(g/cm³).

[e] Length of each segment: 25.4 mm.

[f] Length of each segment: 50.0 mm.

Firing data for the 17-mm rate stick showed that the first section was slightly overboosted and detonated with an overall velocity of 6.103 mm/μs. The next two sections (5.9 diameters in overall length) detonated with an average velocity of 6.029 mm/μs. The last section failed to detonate completely and thus 17 mm is very close to the failure diameter.

The diameter-effect curve was obtained by least-squares fitting the data from the four rate sticks with the form

$$D = D_i \left[1 - \frac{A}{(R - R_c)} \right],$$

where D is the observed detonation velocity of a stick of radius R, D_i is the extrapolated value of the detonation velocity for a charge of indefinitely large radius, and A and R_c are fitting parameters. Results of the fitting are listed in Table IV and the experimental data and the fitted curve are plotted in Fig. 6.

(2) Initiation Tests with Amatex/20. Four important factors in shock initiation of explosives are the amplitude and duration of the initiating shock, the area shocked, and the divergence of flow behind the shock wave. The first two of these factors were utilized by Ramsay and Popolato[4] to order the shock sensitivities of various explosives through the relationship between time-to-detonation and the input shock strength. These two factors were also used by Walker and Wasley[5] in developing the "critical initiation energy" as a measure of sensitivity.

In the present work, data are being obtained for the run-to-detonation in Amatex/20 using the wedge technique. These data will be useful in understanding the initiation behavior of this explosive as compared to other military explosives. The data will also be useful in detecting variations in sensitivity that result from variation of AN particle size or from other causes. They will also be useful for determining the unreacted Hugoniot

TABLE IV

DIAMETER-EFFECT CURVE FOR AMATEX/20 PREPARED FROM CRUSHED AN PRILLS[a]

Fitting Form: $D = D_i [1 - A/(R - R_c)]$

Constant	Value	Standard Deviation
D_i	7.030 mm/μs	0.010 mm/μs
A	0.585 mm	0.031 mm
R_c	4.390 mm	0.196 mm

Charge Diameter (mm)	Observed Velocity (mm/μs)	Calculated Velocity (mm/μs)	Deviation $(V_{OBS} - V_{CALC}) \times 10^3$ (mm/μs)
101.6	6.937	6.941	-4
50.8	6.840	6.834	6
25.4	6.532	6.535	-3
17.0	6.029	6.029	0

[a] AN median particle diameter: ~500 μm.

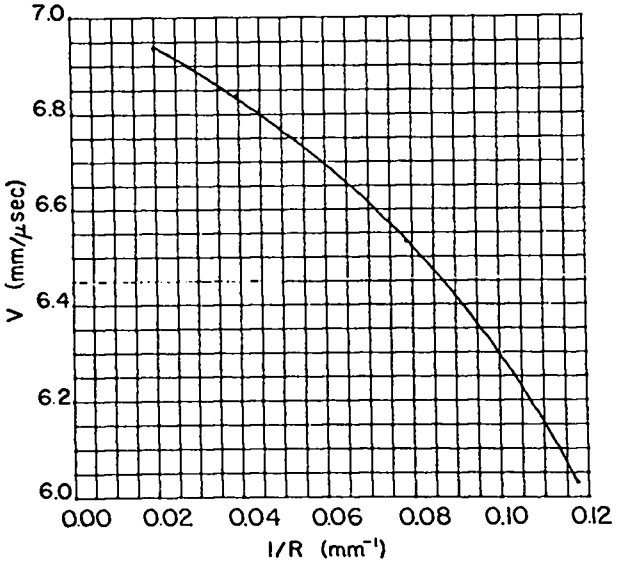

Fig. 6. Plot of detonation velocity data for rate sticks of Amatex/20 prepared with crushed AN. Density: 1.613 g/cm³. The curve is a result of a least-squares fit to the data using the expression $D = D_i[1 - A/(R - R_c)]$.

curve for Amatex and the dependence of this curve on composition.

Despite the value of these data, no theoretical or empirical relationship exists for proceeding from such data to the prediction of the performance of military boosters. The performance of these boosters is strongly affected by the third and fourth factors mentioned above - the area over which the initiating shock is transmitted and the radius of curvature of the shock front. Work by Johansson and Sjölin[6] and unpublished work at LASL on initiation with divergent shock waves have shown that the induced shock may have an initial amplitude of only a few tens of kilobars and yet, initiation can be successful; that as the area and radius of curvature of the induced shock wave are decreased, the initial pressure must be increased, even beyond the detonation pressure of the acceptor explosive (as in the case of jet attack); that weak initiation may result in the formation of a detonation wave that is axially directed and propagates laterally after some delay; that neither the shock velocity nor the occurrence of detonation reaction over a portion of the shock front is a sufficient criterion for detonation to propagate.

Many munitions in which it is proposed to use Amatex presently employ small boosters sized to initiate detonation in the preferred fill with a diameter not far from the failure diameter of Amatex/20 (Table V). All these boosters are "point" initiated, and at times, a barrier of inert material is interposed between the booster pellet and the acceptor charge. All these factors - small diameter, point initiation, interposed barrier - make initiation of Amatex/20 more uncertain.

To probe the problem of initiation of Amatex/20 when the above-mentioned factors were present, a few experiments were performed with booster pellets of PBX 9407 with the following dimensions:

PBX 9407 Booster Pellet Dimensions

Diameter (mm)	Height (mm)	Density (g/cm^3)
19.05	6.35	1.67
38.10	12.70	1.67

TABLE V[a]

SOME CURRENT FUZE BOOSTERS

Fuze	Used in	Booster (mm) Diameter	Booster (mm) Height	Booster Explosive	Explosive Density (g/cm^3)
M557	90-mm shell	38.86	12.52	Comp. A-5	1.50 - 1.70
	105-mm shell	"	"		
M582	155-mm shell	"	"		
	175-mm shell	"	"		
	8-in. shell	-	-		
	4.2-in. mortar	38.86	12.52		
M732	105-mm shell	21.97	9.601	Comp. CH-6	1.62 - 1.67
	155-mm shell	-	-		
	175-mm shell	-	-		
	8-in. shell	-	-		
	4.2-in. mortar	-	-		
--	BLU-63	14.91	5.207	RDX or Comp. A-5	1.55

[a]Most of these data were supplied by D. E. Seeger, PA, in a private communication to B. G. Craig.

This explosive is composed of RDX and Exon 461* in the weight ratio 94/6 and has a detonation pressure of 287 kbar at a density of 1.67 g/cm^3.[7]

Two techniques were employed to assess the quality of initiation. First, the transit time through the acceptor was measured using thin foil pin switches. Initiation may be assumed to be prompt if, for a thin charge, the observed detonation velocity is about equal to that of a stick of Amatex having a diameter equal to that of the booster. Second, the emergence of the detonation from the acceptor charge was observed with a rotating mirror camera. Prompt initiation was indicated by emergence of the detonation from the side of the acceptor at a point near the surface of shock entry, poor initiation by more distant emergence.

The first type of experiment performed is described in Fig. 7 and the associated tables. A PBX 9407 booster pellet of each size was placed in direct contact with an acceptor disk of Comp. B-3 (ρ = 1.73 g/cm^3) and detonated with a detonator having a diameter of 7.62 mm. Detonation velocity of the Comp. B-3 under the small pellet was 7.627 mm/μs and under the large pellet, 7.674 mm/μs. These values compare favorably with the expected detonation velocity of this explosive at the diameters of interest, 7.990 mm/μs, and the transit times indicate an excess time of only 0.07 μs. Detonation was observed to spread laterally promptly, emerging from edges of the Comp. B-3 disk at a distance of only 3mm from the initial surface. These results indicate that these booster pellets initiate detonation in Comp. B promptly.

The experiment was repeated with an acceptor disk of Amatex/20 substituted for the Comp. B-3. Detonation under the large pellet traversed the disk at an average velocity of 6.261 mm/μs and spread laterally fairly promptly, emerging at the edge at a distance of 6 mm from the initial surface. Detonation under the smaller pellet traversed the disk at

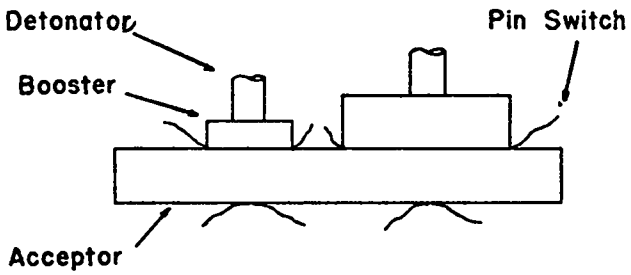

Fig. 7. Booster Sensitivities of Amatex/20. Detonator diameter: 7.62 mm.

TEST GEOMETRY

Booster		
Size	Small	Large
Explosive	PBX 9407	PBX 9407
Density (g/cm^3)	1.67	1.67
Diameter (mm)	19.05	38.10
Height (mm)	6.36	12.70
Acceptor Disk		
Explosive	Comp. B-3	Amatex/20
Density (g/cm^3)	1.73	1 613
Diameter (mm)	101.60	101.60
Height (mm)	12.51	12.48

TEST RESULTS

	Transit Time (μs)		Detonation Velocity (mm/μs)	
Booster size	Small	Large	Small	Large
Comp. B-3	1.64	1.63	7.627	7.674
Amatex/20	2.248 2.255	1.99	5.553 5.536	6.261

an average velocity of only 5.553 mm/μs - a value well below that exhibited by a rate stick of slightly more than failure diameter. Moreover, detonation did not spread laterally. This experiment was repeated using only the smaller booster pellet, and again detonation failed to propagate laterally. The average detonation velocity through the Amatex/20 was measured to be 5.536 mm/μs - a value in good agreement with the first result.

To further evaluate the smaller pellet, the experiment, shown schematically in Fig. 8, was performed and gave the rotating-mirror camera record shown in Fig. 9. Average detonation

*A product of Firestone Plastics Company.

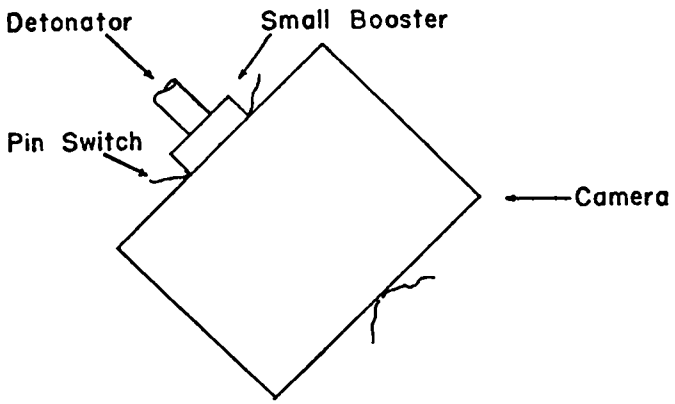

Fig. 8. Booster sensitivity test. Detonator diameter - 7.62 mm.

TEST GEOMETRY

	Small Booster	Acceptor Cylinder
Explosive	PBX 9407	Amatex/20
Density (g/cm^3)	1.67	1.613
Diameter (mm)	19.05	66.60
Height (mm)	6.35	50.87

TEST RESULTS

Transit time (μs)	8.35
Detonation velocity (mm/μs)	6.092
Breakout below top (mm)	20.5

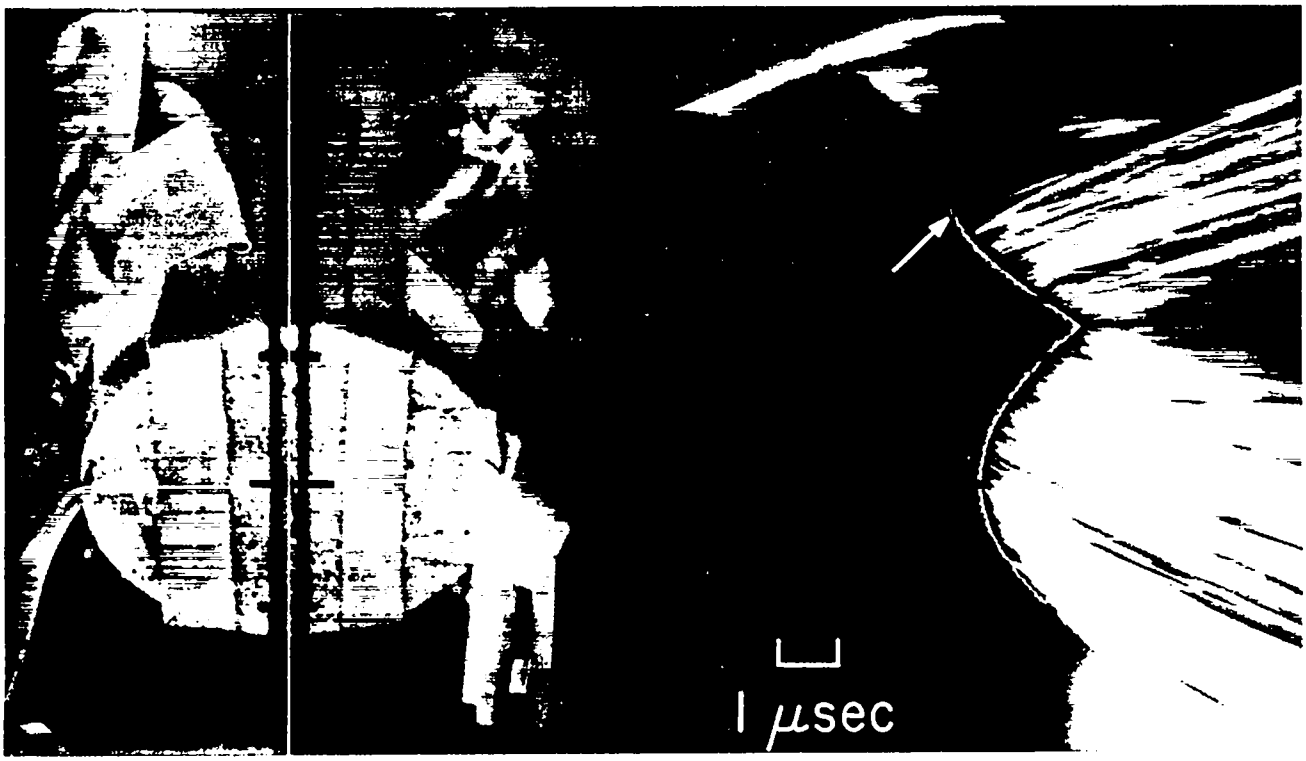

Fig. 9. Left: Still photograph of Amatex cylinder as viewed by rotating-mirror camera. The camera slit position is shown by the white vertical line. The booster pellet was located on the upper plane surface of the cylinder. Right: Detonation record. Time increases to the right. The white arrow indicates breakout of detonation at the cylinder wall.

velocity (6.092 mm/μs) and side breakout distance (20.5 mm) indicate that the small PBX 9407 booster pellet is marginal in its ability to initiate Amatex/20.

The performance of the large booster pellet in initiating Amatex/20 through a layer of steel corresponding to the combined thicknesses of the XM-732 booster cup and fuze-cavity liner, 3.02 mm, was tested as shown in Fig. 10. The average detonation velocity through the acceptor charge and the large breakout distance suggest that this large booster is marginal for initiating Amatex/20, although performance might be improved if the pellet and barrier were embedded in the acceptor explosive.

c. Relative Energy of Amatex

The cylinder test involves observation of the expansion of the wall of a tube of ductile copper driven by the detonation products of a closely fitted core of explosive. Results can be used to compare the efficiencies of different explosives for imparting kinetic energy to metal. In the work reported here, the efficiency of Amatex is compared with that of the military preferred fill explosive, Comp. B Grade A.

When the cylinder test is applied to high-energy secondary explosives such as Comp. B and TNT, the results are observed to scale within the accuracy of the technique, which is about one percent, i.e., if the inside radius of the cylinder is scaled by a factor, S, relative to a reference cylinder loaded with the same explosive, then the wall velocity at a radial expansion of $S(R - R_o)$ is equal to that obtained for the reference cylinder at an expansion of $R - R_o$, and the time required for an expansion of $S(R - R_o)$ is S times as great as the time for an expansion of $R - R_o$ by the reference cylinder. In the work reported here, the inside diameter of the cylinders was nominally 101.6 mm; the results are scaled to an inside diameter of 25.4 mm for comparison.

In order for scaling to be observed or for the metal-accelerating capabilities of different explosives to be readily compared, the ratio of casing weight to charge volume must be kept constant at some common value. At Lawrence Livermore Laboratory (LLL), a large quantity of cylinder-test data have been developed using a loading of 4.0291 to 4.0331 g of copper per cubic centimeter of explosive. The value 4.0331 was used in the work reported here.

For the tests reported below, the copper tubes were loaded with explosive in the form of right circular cylinders accurately machined. During loading, any external flaws in the explosive were repaired by filling with a paste of RDX and oil or with XTX 8003. Copper tubes were 889 mm long

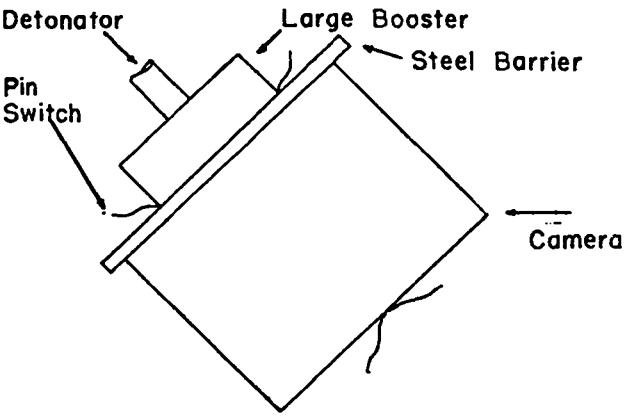

Fig. 10. Sensitivity test - steel barrier. Detonator diameter - 7.62 mm.

TEST GEOMETRY

	Large Booster	Acceptor Cylinder
Explosive	PBX 9407	Amatex/20
Density (g/cm^3)	1.67	1.613
Diameter (mm)	38.10	66.65
Height	12.70	50.76

Steel Barrier

Diameter (mm)	76.2
Height (mm)	3.01

TEST RESULTS

Transit time (μs)	10.02
Detonation velocity (mm/μs)	5.066
Breakout below top (mm)	30.6

and observations were made with a rotating-mirror camera aligned at a point six diameters from the booster end. Detonation velocity was monitored by means of pin switches made of 51-μm enameled magnet wire attached to the outside of each tube at accurately measured intervals of approximately 76 mm.

Analysis of the distance-time data was performed in two ways. For comparison purposes, the 500 to 600 X-T data points were least-squares fitted with a seventh-order polynomial. To bring out the fine detail of the wall motion, the data were fitted with least-squares cubic splines. The spline fit is shown in Fig. A-1 of the Appendix. In this method, the data were divided into 39 groups by use of 40 points, called knots, equally spaced in time. Each group of data points was least-squares fitted with a cubic equation with the constraints that at each knot, adjacent cubics must pass through the same point and have equal values of the first and second derivatives.

Cylinder tests fired to date include Comp. B Grade A, Amatex/20, and Amatex/40. Both the Amatex formulations were prepared with ground prills of AN. The results of these cylinder tests are graphically presented in Figs. 11, 12, and 13, and additional tables and graphs are presented in the Appendix. Figure 13 shows the wall kinetic energies relative to Comp. B Grade A taken as 1.00, scaled to 25.4-mm i.d. The curves for Amatex/20 and Amatex/40 show increased acceleration starting at an expansion of about 90 mm (22.5 mm scaled) and an increased wall kinetic energy relative to Comp. B. This behavior has also been observed for one cylinder test on an Amatex containing prilled AN, but the late acceleration of the cylinder wall was not so pronounced. Figure 13 is plotted from data contained in Tables A-II and A-III. From these tables, we find that Amatex/20, at the customary reference expansion of 19 mm (scaled to 25.4 mm), imparts to the cylinder wall 82% as much energy as does Comp. B Grade A, and Amatex/40, 93%. These data are in agreement with the data obtained by Hershkowitz and Rigdon.[8]

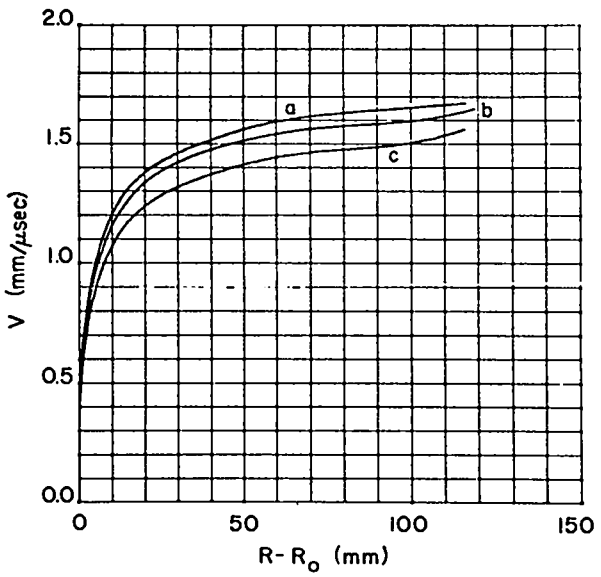

Fig. 11. Velocity vs expansion radius for the 101.4-mm cylinder tests. Graphs a, b, and c correspond to Comp. B Grade A, Amatex/40, and Amatex/20, respectively.

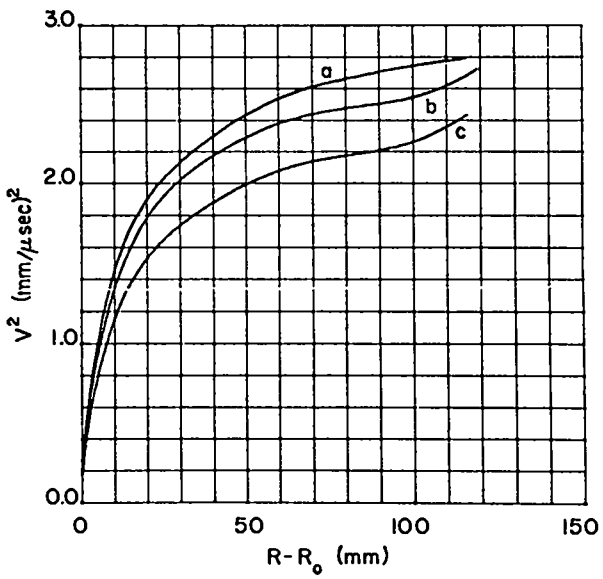

Fig. 12. Specific wall kinetic energy vs expansion radius for the 101.4-mm cylinder tests. Graphs a, b, and c correspond to Comp. B Grade A, Amatex/40, and Amatex/20, respectively.

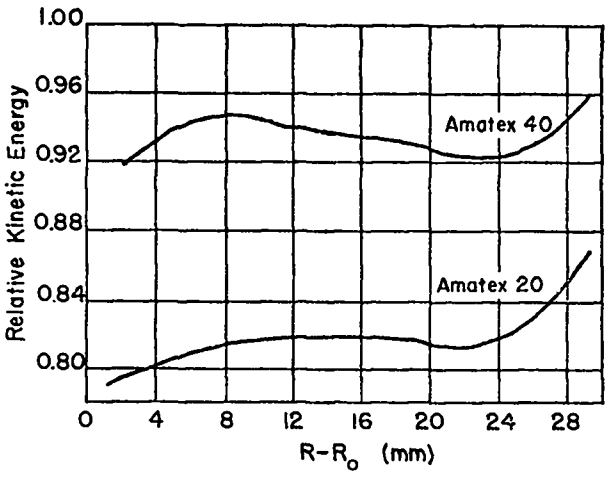

Fig. 13. Kinetic energy imparted to the cylinder wall (normalized to Comp. B Grade A) vs expansion radius for the 101.4-mm cylinder tests of Amatex/20 and Amatex/40.

3. Future Work

Work on the shock initiation of Amatex as a function of composition and AN granulation is in progress. Results of this study are applicable to the design of the booster system. A 101.4-mm-diam cylinder test loaded with Amatex/20 prepared with prills has been fired and these data are being analyzed. Work with the AN-KN system should be started to determine the effect of KN addition on the dimensional stability of the cast charge, and to determine other properties of interest.

B. ANALYSIS OF PREMATURES (TASK B), C. A. Anderson, A. D. Randolph

1. Introduction

One likely cause of in-bore prematures is the rapid closure of an air gap in the base of the ammunition. The closure of the gap leads to compression heating, thermal transport, and thermal ignition. This mechanism was modeled and our initial attempts to calibrate the model with simulated setback experiments conducted in an aquarium test were not successful. Our work for the past quarter has been devoted to a recalibration of the model with a better thermal transport calculation.

2. Progress This Report Period

Thermal Model for the Aquarium Gap Ignition Tests

The experimental gap ignition tests described in detail in a previous quarterly report[1] were further analyzed with a sophisticated thermal transport computer program. This program, NEWGAP, was developed at the University of Arizona under AFOSR Contract F44620-70-C-0080 for the study of accidental initiation of HE in encased weapons systems. This program simulates the closure of a gas-filled gap between planar HE and inert surfaces, Plexiglas/gas/TNT, in the aquarium experiments. The gap is assumed to compress with an arbitrary pressure-time profile, P(t), thus raising the temperature, and transferring heat to the surrounding walls. Continuity of temperature and thermal flux are assumed across the gas/HE and gas/inert interfaces. The physical model is similar to the gap compression model described previously.[9]

Program NEWGAP solves the one-dimensional, transient, reactive heat equation in the three media with suitable boundary and initial conditions. Ignitions were assumed to occur when the HE reaction kinetics liberated sufficient energy to raise the first interior HE mesh point above the hot gas/HE surface temperature, thus indicating that the rate of energy generation in the HE exceeded the rate of energy transfer. Very large thermal gradients, e.g., 1000 K/μm, were calculated for the rapid compression times characteristic of the aquarium tests. Program NEWGAP utilizes an efficient numerical algorithm that permits small meshing with second order accuracy in the high gradient regions near boundaries. This program permits a more realistic evaluation of thermal transport processes in these low amplitude shock gap compression tests.

Calculations with Program NEWGAP indicate that surface ignition by gas compression is a plausible explanation for the surface ignitions that were observed in the aquarium tests. Ignition

calculations were carried out with the parameter values shown in Table VI. In these calculations, the gas pressure was represented by the simple power-law equation

$$P(t) - \left(P_m - P_o\right)\left(t/t_c\right)^n + P_o \ .$$

This empirical equation, used in Program NEWGAP to introduce the compression heating event into the thermal transport equation, gave a good fit to P(t) for the aquarium shots calculated from the SIN hydrocode by Mader.[10] Thermal ignitions were relatively independent of the parameters, n and t_c (indicating that the compression was nearly adiabatic), but depended on the peak pressure P_m. Table VII shows the calculated critical gap width as a function of assumed peak pressure and TNT thermal conductivity for the three gases used in the experimental tests.

In the aquarium shots, all gap thicknesses used (ranging from 1 to 5 mm) produced ignitions on bare TNT surfaces. The calculated critical gap values shown in Table VII for air and krypton are in agreement with these experimental data. However, calculations using the properties of methane indicate that lower TNT thermal conductivity and/or higher peak pressure and/or more sensitive reaction kinetics would be required to produce ignition with a 1.0-mm gap. In addition, methane thermal conductivity at 2 kbar would be expected to increase above the perfect gas values (corrected for temperature) used in these calculations.

These results suggest that there may be a mechanism for concentration of thermal energy at the gas/HE surface. Two possible mechanisms that would result in easier HE ignition by gas compression are:

- Individual low conductivity crystals due to possible anisotropy of thermal conductivity and random orientation of crystal axes
- Three-dimensional heat transfer around surface asperities

3. Future Work

Further tests with the aquarium apparatus will attempt to better characterize the HE surface, thus identifying points of surface ignition with surface defects. Tests will also be made with the TNT test samples placed at a larger radius from the initiating charge in an attempt to span the critical ignition gap width for the various gases. This critical gap width was spanned in one series of shots in the original tests when a thin foil of aluminum was glued to the face of the HE. This configuration produced ignition with a 5-mm air gap, but none with a 1-mm air gap. Program NEWGAP will be modified to simulate this test situation.

TABLE VI

BASE-LINE PARAMETER VALUES USED IN NEWGAP THERMAL IGNITION STUDY

Parameter	Value
Activation energy, ΔE (kJ/g-mol)	172
Preexponential factor, A (g-mol/s-m^3)	1.12×10^{17}
Characteristic time, t_c (μs)	1.15
Peak pressure, P_m (MPa)	200, 340, or 500
Pressure exponent, n	11.4
Thermal conductivity, k_{TNT} (W/m-K)	0.26

TABLE VII

CALCULATED CRITICAL GAP WIDTHS TO IGNITE TNT (mm)

P_{max}	Air		Methane		Krypton	
	k_{TNT} (W/m-K)					
(MPa)	0.26	0.13	0.26	0.13	0.26	0.13
200	-	-	-	(6.4)[a]	1.39	0.37
340	1.58	0.50	9.1	2.62 (1.03)	0.27	-
500	0.58	-	-	0.97	-	-

[a] ( ) calculations using ten-fold increase in TNT decomposition frequency factor.

In addition to completing this study on the gas compression mechanism, we expect to have our first numerical results on the void collapse mechanism discussed in the first quarterly progress report.[9]

C. SYNTHESIS OF HMX (TASK C)

Funds allocated to this task were expended during the first two quarters, and results were reported in the first and second quarterly reports.

Additional work is being conducted with funds provided by PA.

D. INITIATION AND SENSITIVITY (TASK D)
B. G. Craig

1. Introduction

The ultimate objective of this investigation is to obtain a quantitative understanding of the mechanisms leading to the initiation of a violent reaction in the high explosive. One approach to developing a quantitative model of the initiation is to study the response of an explosive subjected to a single shock of known amplitude and duration in a one-dimensional system. This requires the development of a plane wave shock generator and supporting instrumentation for experiments that will generate data that can be used to determine the state of the shocked explosive as a function of time and initial conditions.

2. Progress This Report Period

Our problem to date has been the design of a satisfactory flyer plate plane wave generator. We have traced part of the problem related to the design of the flyer plate plane wave shock generator to the method used to bond the sheet explosive to the aluminum flyer. Small air gaps between the explosive and aluminum caused large timing errors. Techniques are being developed to improve the bonding procedure.

3. Future Work

Work will continue on the design of plane wave generators and the instrumentation required to measure the amplitude and duration of the shock pulse.

REFERENCES

1. A. Popolato, "Joint Services Explosive Program," Los Alamos Scientific Laboratory report LA-5616-PR (May 1974).

2. A. W. Campbell, M. E. Malin, T. J. Boyd, Jr., and J. A. Hull, "Precision Measurement of Detonation Velocities in Liquid and Solid Explosives," Rev. Sci. Instrum. 27, 567-574 (1956).

3. A. Popolato, A. W. Campbell, L. W. Hantel, H. R. Lewis, P. G. Salgado, and B. G. Craig, "Properties of Amatex/20," Los Alamos Scientific Laboratory report LA-5516-MS (March 1974). (Work performed for Picatinny Arsenal with funds provided under MIPR-3311-1028.)

4. J. B. Ramsay and A. Popolato, "Analysis of Shock Wave Initiation for Solid Explosives," Proc. 4th Symp. (Intern.) on Detonation, U.S. Naval Ordnance Laboratory, White Oak, Maryland, October 12-15, 1965, pp. 233-238.

5. F. E. Walker and J. R. Wasley, "Critical Energy for Shock Initiation of Heterogeneous Explosives," Explosivstoffe 1, 9-13 (1969).

6. C. H. Johansson and T. Sjölin, "The Initiation Properties of Boosters in Explosives with Low Sensitivity," Proc. 4th Symp. (Intern.) on Detonation, U.S. Naval Ordnance Laboratory, White Oak, Maryland, October 2-15, 1965, pp. 435-441.

7. B. M. Dobratz, Ed., "Properties of Some Chemical Explosives and Explosive Simulants," Lawrence Livermore Laboratory report UCRL-51319 (December 1972).

8. J. Hershkowitz and J. Rigdon, "Evaluation by a Modified Cylinder Test of Metal Acceleration by Non-Ideal Explosives Containing Ammonium Nitrate," Picatinny Arsenal report PATR 4611 (April 1974).

9. A. Popolato, "Joint Services Explosive Program," Los Alamos Scientific Laboratory report LA-5402-PR (September 1973).

10. A. Popolato, "Joint Services Explosive Program, Los Alamos Scientific Laboratory report LA-5521-PR (March 1974).

APPENDIX

The cylinder test copper wall expansions for Comp. B, Amatex/40, and Amatex/20 are given in Tables A-I, A-II, and A-III. The velocity expansion curve for Comp. B is shown in Fig. A-1.

TABLE A-I

CYLINDER TEST,
CAST COMP. B GRADE A

Density 1.701 g/cm^3; Loading Factor 4.0331 g/cm^3
Values scaled to 25.4 mm i.d.
using a scale factor of 3.979

Observed Expansion $R - R_o$ (mm)	Scaled Expansion $R - R_o$ (mm)	Scaled Time T (μs)	V^2 (mm/μs)^2
3.979	1	1.299	0.874
7.958	2	2.258	1.291
11.937	3	3.093	1.566
15.916	4	3.868	1.756
19.895	5	4.607	1.895
23.874	6	5.323	2.002
27.853	7	6.022	2.089
31.832	8	6.708	2.164
35.811	9	7.382	2.232
39.790	10	8.047	2.294
43.769	11	8.703	2.352
47.748	12	9.351	2.405
51.727	13	9.993	2.453
55.706	14	10.629	2.497
59.685	15	11.259	2.535
63.664	16	11.885	2.567
67.643	17	12.507	2.595
71.622	18	13.127	2.619
75.601	19	13.745	2.643
79.580	20	14.358	2.667
83.559	21	14.970	2.686
87.538	22	15.579	2.703
91.517	23	16.186	2.718
95.496	24	16.972	2.731
99.475	25	17.396	2.744
103.454	26	17.999	2.756
107.433	27	18.601	2.768
111.412	28	19.201	2.780
115.391	29	19.800	2.793

TABLE A-II

CYLINDER TEST, OPEN MELT,
AMATEX/40 MADE WITH GROUND AN PRILLS

Density 1.652 g/cm^3; Loading Factor 4.0331 g/cm^3
Values scaled to 25.4 mm i.d.
using a scale factor of 3.975

Observed Expansion $R - R_o$ (mm)	Scaled Expansion $R - R_o$ (mm)	Scaled Time T (μs)	V^2 (mm/μs)^2	$\frac{V^2}{V^2_{CB}}$ [a]
3.975	1	1.342	0.812	0.929
7.950	2	2.341	1.185	0.918
11.925	3	3.211	1.447	0.924
15.900	4	4.015	1.637	0.932
19.875	5	4.780	1.779	0.939
23.850	6	5.518	1.890	0.944
27.825	7	6.237	1.978	0.947
31.800	8	6.941	2.051	0.948
35.775	9	7.634	2.114	0.947
39.750	10	8.317	2.169	0.946
43.725	11	8.992	2.219	0.943
47.700	12	9.660	2.264	0.941
51.675	13	10.322	2.305	0.940
55.650	14	10.978	2.341	0.938
59.625	15	11.629	2.373	0.936
63.600	16	12.276	2.402	0.936
67.575	17	12.920	2.425	0.934
71.550	18	13.560	2.445	0.934
75.525	19	14.198	2.462	0.932
79.500	20	14.835	2.476	0.928
83.475	21	15.470	2.488	0.926
87.450	22	16.103	2.499	0.925
91.425	23	16.735	2.511	0.924
95.400	24	17.365	2.524	0.924
99.375	25	17.994	2.542	0.926
103.350	26	18.619	2.565	0.931
107.325	27	19.242	2.594	0.937
111.300	28	19.861	2.631	0.946
115.275	29	20.475	2.676	0.958

[a] Wall kinetic energy relative to Comp. B Grade A.

TABLE A-III

CYLINDER TEST, OPEN MELT,
AMATEX/20 MADE WITH GROUND AN PRILLS

Density 1.613 g/cm^3; Loading Factor 4.0331 g/cm^3
Values scaled to 25.4 mm i.d.
using a scale factor of 3.988

Observed Expansion $R - R_o$ (mm)	Scaled Expansion $R - R_o$ (mm)	Scaled Time T (μs)	V^2 (mm/μs)^2	$\frac{V^2}{V^2_{CB}}$ [a]
3.988	1	1.4961	0.691	0.791
7.976	2	2.573	1.054	0.816
11.964	3	3.510	1.249	0.798
15.952	4	4.376	1.410	0.803
19.940	5	5.201	1.529	0.807
23.928	6	5.997	1.623	0.811
27.916	7	6.772	1.700	0.814
31.904	8	7.532	1.765	0.816
35.892	9	8.278	1.824	0.817
39.880	10	9.013	1.877	0.818
43.868	11	9.738	1.926	0.819
47.856	12	10.455	1.971	0.820
51.844	13	11.163	2.011	0.820
55.832	14	11.865	2.047	0.820
59.820	15	12.561	2.079	0.820
63.808	16	13.253	2.106	0.820
67.796	17	13.940	2.128	0.820
71.784	18	14.624	2.146	0.819
75.772	19	15.305	2.161	0.818
79.760	20	15.984	2.174	0.815
83.748	21	16.661	2.187	0.814
87.736	22	17.337	2.200	0.814
91.724	23	18.010	2.215	0.815
95.712	24	18.680	2.234	0.818
99.700	25	19.348	2.259	0.823
103.688	26	20.011	2.291	0.831
107.676	27	20.669	2.330	0.842
111.664	28	21.320	2.377	0.855
115.652	29	21.966	2.430	0.870

[a] Wall kinetic energy relative to Comp. B Grade A.

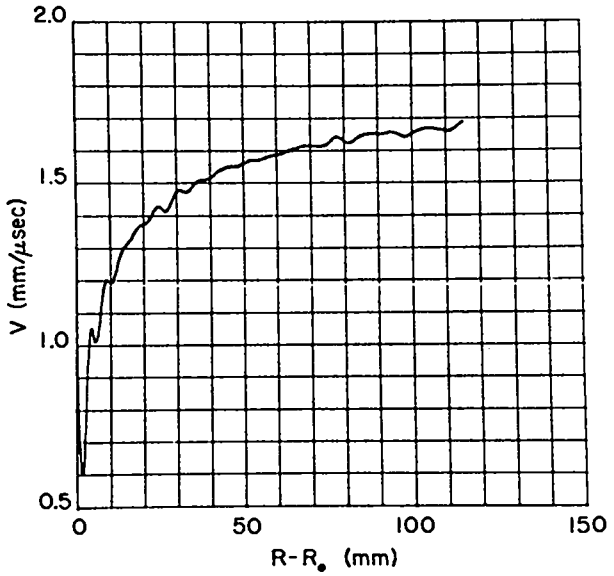

Fig. A-1. Velocity vs expansion radius for the 101.4-mm Comp. B cylinder test. A forty-knot spline fit was used in the data reduction. The explosive density was 1.701 g/cm^3 and the loading factor 4.0331 g/cm^3.

ALT:100(70)

DISTRIBUTION	No. of Copies
Director DARPA, Attn: Program Management, Arlington, VA 22209	3
Charles Ravitsky, DARPA, Arlington, VA 22209	1
Ray Thorkildsen, DDR&E, The Pentagon, Washington, D.C. 20301	1
F. E. Walker, LLL, Livermore, CA 94550	2
R. F. Walker (SMUPA-FR-E), Picatinny Arsenal, Dover, NJ 07801	2
H. J. Matzuguma (SARPA-FR-E-C), Picatinny Arsenal, Dover, NJ 07801	1
L. W. Saffian (SMUPA-MT), Picatinny Arsenal, Dover, NJ 07801	1
D. E. Seeger, Explosives Application Section, Picatinny Arsenal, Dover, NJ 07801	1
J. R. Hendrickson, Sr. (SARPA-FR-E-A), Picatinny Arsenal, Dover, NJ 07801	1
Maj. Gen. Ernest Graves/D. I. Gale, DMA, USAEC, Washington, D.C. 20545	1
H. J. Gryting, NWC, China Lake, CA 93555	1
A. B. Amster, NOSC, Washington, D.C. 20360	1
J. E. Ablard, NOL, Silver Spring, MD 20910	1
D. Price, NOL, Silver Spring, MD 20910	1
M. Kamlet, NOL, Silver Spring, MD 20910	1
C. Boyars, NOL, Silver Spring, MD 20910	1
M. F. Zimmer, AFATL/DLDE, Eglin AFB, FL 32542	1
D. K. Nowlin/M. D. Roepke, USAEC ALO, Albuquerque, NM 87115	1
Capt. R. R. McGuire, FJSRL, USAF Academy, Colorado Springs, CO 80840	1
P. M. Howe (AMXRD-OD), BRL, APG, Aberdeen, MD 21005	1
INTERNAL LASL DISTRIBUTION	
D. P. MacDougall	1
A. D. McGuire	1
E. H. Eyster	1
M. L. Brooks	1
W. E. Deal	1
J. R. Travis/B. G. Craig/A. W. Campbell/R. P. Engelke	4
P. A. Carruthers/C. L. Mader	2
L. C. Smith/M. D. Coburn/H. H. Cady/T. M. Benziger	4
J. Aragon/A. Popolato/C. A. Anderson/T. Rivera/A. D. Randolph	5